



Some aspects of beech biomechanics: juvenile wood properties, sapwood pre-stress and growth forces

Delphine Jullien, Shengquan Liu, Caroline Loup, Joseph Gril, Bernard Thibaut

► To cite this version:

Delphine Jullien, Shengquan Liu, Caroline Loup, Joseph Gril, Bernard Thibaut. Some aspects of beech biomechanics: juvenile wood properties, sapwood pre-stress and growth forces. 2023. hal-04133248v1

HAL Id: hal-04133248

<https://hal.science/hal-04133248v1>

Preprint submitted on 19 Jun 2023 (v1), last revised 1 Jul 2023 (v2)

HAL is a multi-disciplinary open access archive for the deposit and dissemination of scientific research documents, whether they are published or not. The documents may come from teaching and research institutions in France or abroad, or from public or private research centers.

L'archive ouverte pluridisciplinaire **HAL**, est destinée au dépôt et à la diffusion de documents scientifiques de niveau recherche, publiés ou non, émanant des établissements d'enseignement et de recherche français ou étrangers, des laboratoires publics ou privés.

Some aspects of beech biomechanics: juvenile wood properties, sapwood pre-stress and growth forces.

JULLIEN Delphine¹, LIU Shengquan², LOUP Caroline³,
GRIL Joseph^{4,5,*}, THIBAUT Bernard¹

¹ LMGC, Univ Montpellier, CNRS, Montpellier, France

² School of Forestry & Landscape Architecture, Anhui Agricultural University, Hefei, China.

³ Service du Patrimoine Historique, Univ Montpellier, Montpellier, France

⁴ Université Clermont Auvergne, CNRS, Institut Pascal, Clermont-Ferrand, France

⁵ Université Clermont Auvergne, INRAE, PIAF, Clermont-Ferrand, France

* Corresponding author, email : joseph.gril@cnrs.fr

Keywords

Beech; Growth stress; Wood properties; Variability; Radial variation

Abstract

The building of a tree is the result of wood growth through successive division, expansion and maturation of living cells at the periphery of the trunk and branches. During this process, diameter growth is combined with sapwood pre-stress to allow posture control by the generation of growth forces in the living wood cells. These mechanical aspects of tree building can be characterised at each peripheral position by parameters describing the amount of material produced, wood rigidity and the strain induced by the maturation process. In-situ assessment of maturation strains at the trunk periphery of beech trees, combined with laboratory measurements of ring width (RW), wood density (D) and wood specific modulus (SM), was used to examine biomechanical aspects of juvenility corresponding to young stages of the tree, as well as the correlation or trade-off between sapwood pre-stressing and the generation of forces in the living wood layer used to control tree posture. The radial variations of RW , D and SM , averaged over 86 trees, were close to the “typical radial pattern” of juvenile wood for softwood plantation trees: decrease in RW and increase in D and SM from pith to bark in the juvenile phase. But D only increased in the very first rings, then remained more or less constant. Furthermore, for all three parameters there were many discrepancies in the pattern of variation between trees and even between plots. This is a good indication that the mechanical juvenility of the wood was more related to the biomechanical conditions experienced by the trees in the young ages than to the age of the tree as such (which is the case for fibre length). The level of pre-stress and posture control forces were strongly dependent on the maturation strain as the first explanatory factor. But pre-stress is independent of RW , whereas posture control force is strongly dependent on this growth parameter. This opens the way to trade-offs between these two biomechanical functions of wood fibres.

1. Introduction

Wood growth is the process used for tree building (Thibaut 2019) including simultaneously primary growth by elongation or creation of twigs (bud role) and secondary growth by thickening of existing woody axes (cambium role). Primary growth is mostly assessed by the trunk slenderness relating primary growth (HT, total height) to secondary growth (DBH, diameter at trunk basis) at each growth step. Trunk, as a first-order axis, plays the major role in tree biomechanics and its building process is the most studied, mainly through secondary growth (Fournier et al 1991, Thibaut et al 2001, Alméras & Clair 2016). The variation of growth parameters characterizing wood structure and properties is dependent on tree ontogeny and adaptation to changes in the environment of the tree during its life. Juvenility, in particular, describes the evolution of wood parameters during the early years of tree life. But the environment of the tree (access to light, wind influence, etc.) also changes during the young period of tree growth and mechanical adaptation of wood growth occurs in answer to these changes. In this paper, the data obtained on a large panel of beech trees in the context of a European collaborative program “Stresses in beech” (Becker & Beimgraben 2001) will be exploited to characterize the patterns of radial variation of wood properties. The study will be preceded by the presentation of typical patterns observed in trees according to the literature.

2. State of the art on the spatial variations of wood properties

2.1 Secondary growth descriptors and mechanical parameters

Secondary growth performed by living wood cells (Raven et al 2007, Savidge 2003, Thibaut 2019) consists of the following successive steps: division of the cambium stem cells into daughter cells; expansion of daughter cells until the end of primary wall formation; thickening of the fibre (or tracheid) cell walls until the end of secondary wall formation; lignification of the whole cell wall, including the compound middle lamella; programmed cell death.

During this living period of wood cells, basic wood features are achieved. They can be described by ring width (RW in m), result of combined cell division and expansion, density (D in kg/m^3) expressing cell wall thickening, specific modulus (SM in Mm^2/s^2) determined by the cellulose micro-fibril organisation in the cell wall, and maturation strain (α_m , no unit) resulting from the final polymerization of lignin and other macromolecular processes (Thibaut & Gril 2021).

Some useful mechanical parameters can be calculated from these basic growth descriptors for an elementary growth unit (Fig. 1):

RW (mm): local ring width, used as secondary growth layer width Δr ;

$RS = 10.\Delta\theta.R.RW$ (in cm^2): ring portion surface for a distance to pith R and angular sector $\Delta\theta$;

$RM = RS.D$ (in kg/m): mass per unit length of the ring portion;

$MOE = SM.D$ (in GPa): longitudinal modulus of elasticity;

$\sigma_m = MOE.\alpha_m$ (in MPa): maturation stress, the pre-stressing of the peripheral layer in the sapwood, mostly made of dead fibres or tracheids;

$RF = 100.RS.\sigma_m$ (RF in N): local ring force.

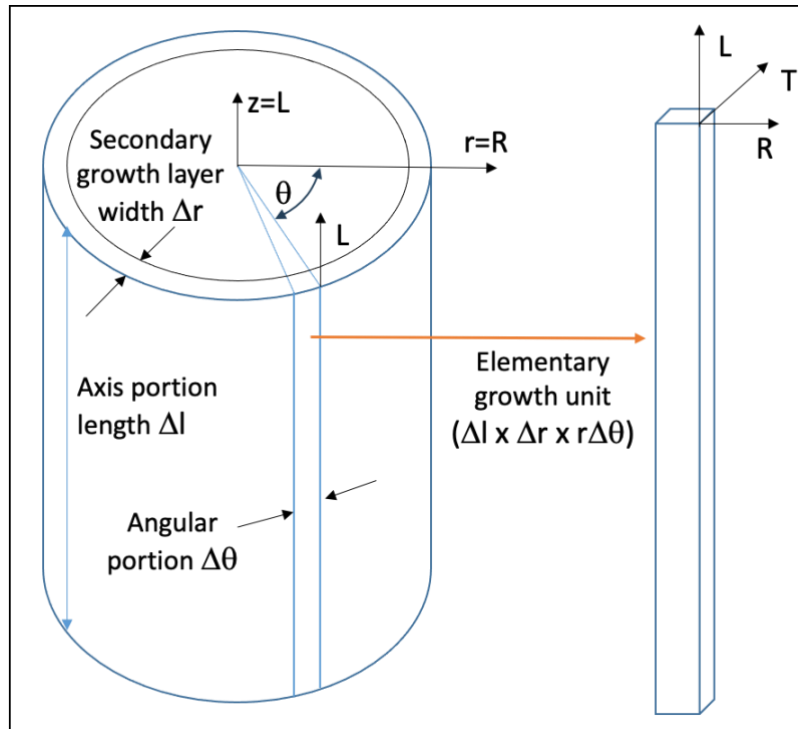


Fig. 1: Local elementary growth unit in a trunk.

(L, r, θ) : cylindrical coordinate system associated to the trunk

(L, R, T): Cartesian coordinate system associated to the elementary growth unit

2.2. Secondary growth variations within a trunk section.

All secondary growth descriptors display spatial variation within a portion of trunk, in the 3 cylindrical directions: transversely across radii (Tar), around the perimeter (Ap) and longitudinally along the stem (Las), called variation “TarApLas” within the tree by Savidge (Savidge 2003). These variations are linked either to the effect of tree age (called juvenility) or to the adaption of the wood growth to external conditions (climate, light availability, accidental leaning ...).

Variations around the perimeter in a given ring are related to a mechanical adaption in the control of posture, i.e. oblique growth in a given direction (in the case of coppice or for the search of light) or progressive change of axis curvature, either to restore verticality after accidental inclination of the tree (Alméras et al 2009) or to change the orientation of the branches after the death of the apex (Fournier et al 1994). Maturation strain asymmetry is the growth parameter most involved in posture regulation (Alméras et al 2005) and there are often large variations between the two sides of the axis (Thibaut & Gril 2021).

The variations along the stem deals with primary growth: i) succession of connected zones and free-from-branching portions of the axis and ii) ageing of the terminal bud in the successive growth unit. Apart from the vicinity of the branching zones, the variations are rather slow (Savidge 2003).

Radial variations, from pith to bark at a given height level can be divided in two types: i) intra-ring short distance changes mostly due to intra-annual climatic changes and ii) variations of mean intra-ring properties linked both to cambium ageing (juvenility) and to the adaption of secondary wood growth to tree mechanics at each growth step (gravity and wind forces depending on tree slenderness and crown development). It is not easy to separate the effects of age per se (time since birth of cambium in the growth unit) and of the mechanical situation of the tree at different growth ages (light availability, wind protection).

The biggest variations in dimensions and environment for a given tree over time occur during the young ages, and so are the variations of wood properties showing higher radial gradients in the inner part of the axis. This inner part, where gradients are monotonously higher (in algebraic value), is called juvenile wood or core wood depending on the authors (Lachenbruch 2011) and their opinion concerning the main factor (juvility or adaptation).

A good description is given in (Bendtsen & Senft 1986) for a softwood and a hardwood. Loblolly pine (Fig. 2) is an example of the typical radial pattern (TRP) of juvenility (Lachenbruch et al 2011): i) initial increase of tracheid length, specific gravity and specific modulus, initial decrease of ring width and microfibril angle (*MFA*); *MFA* variations are closely, negatively related to those of *SM*. This is the general case in softwood plantation trees (Crown & Dowling 2015, Larson et al 2001).

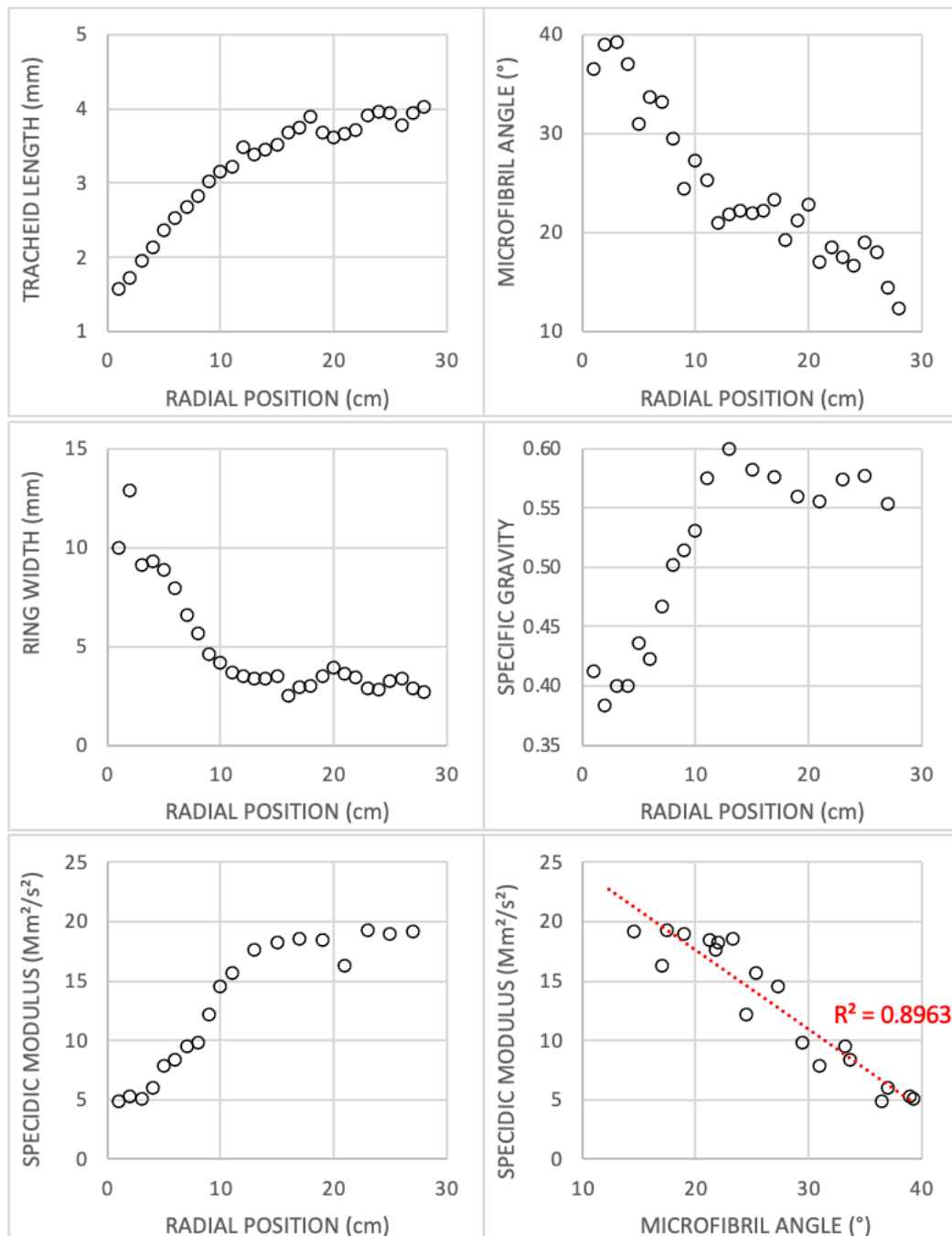


Fig. 2: Radial variations for Loblolly pine, after Bendtsen & Senft (1986).

For Eastern cottonwood (Fig. 3), the ring width initially increases and there is no variation in specific gravity. The variations in fibre length and specific modulus are similar to those of TRP. There is again a highly significant, negative relationship between *MFA* and *SM*.

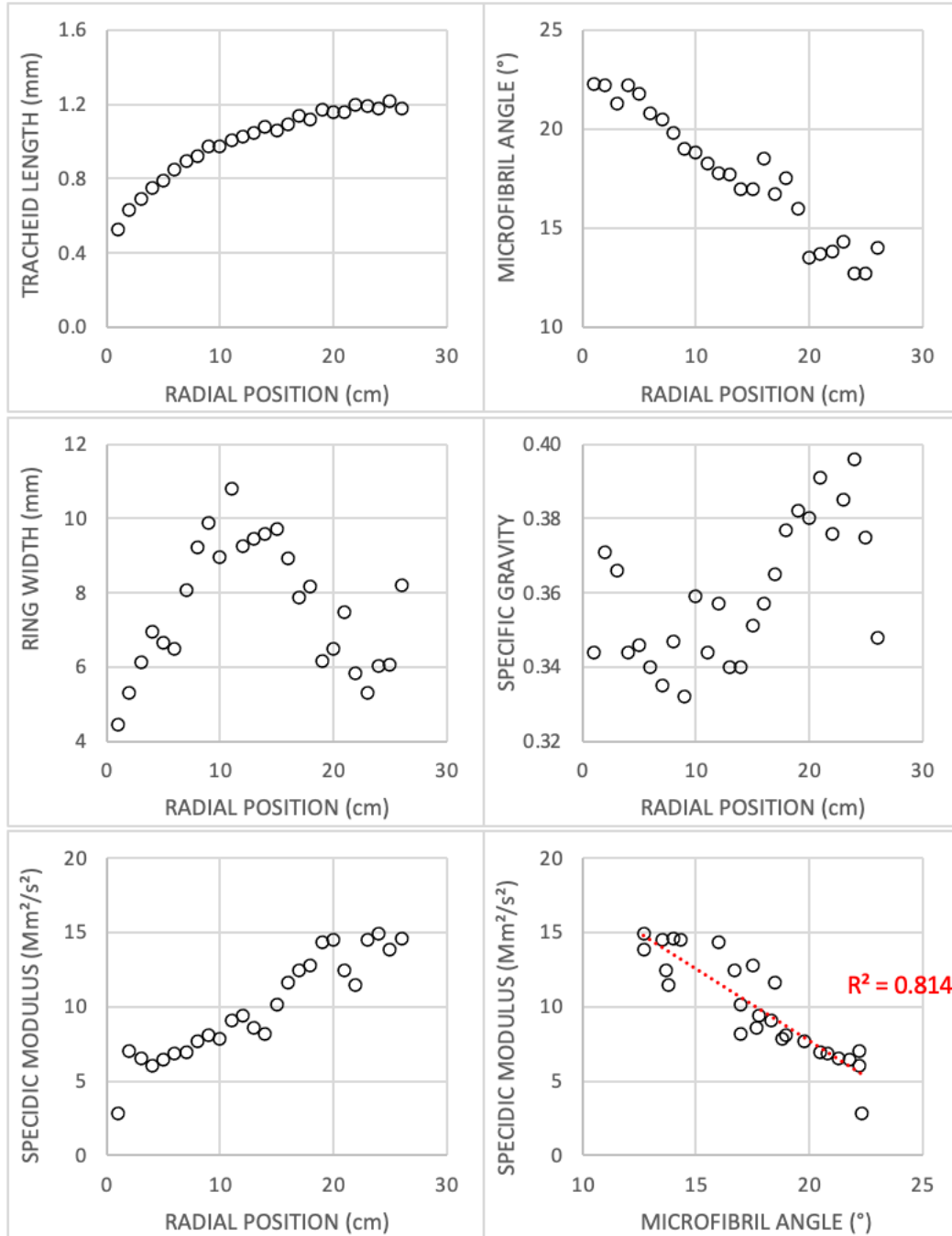


Fig. 3: Radial variations for Eastern cottonwood, after Bendtsen & Senft (1986).

Variations in tracheid or fibre length always share the same initial positive gradient for all trees, whether softwood or hardwood (Koubaa et al 1998, Larson et al 2001, Bhat et al 2001, Bao et al 2001, Kojima et al 2009). This parameter is important for the paper industry (Koubaa et al 1998) but is not cited as a factor influencing the mechanical properties of wood (Kollmann & Côté 1968, Kretschman 2010). The results of initial variations of *RW*, *SG* and *SM* can vary considerably from tree to tree, with flat, positive or negative initial gradients (Bhat et al 2001, Mc Lean et al 2011).

There is very little data on the variation of the average maturation strain within a ring as a function of cambium age or radial position in a log. It has been suggested that the maturation strain can change from positive values (compression stress) in the most juvenile rings compared to negative values (usual tension stress) in older rings, for softwoods (Fournier et al 1990). For hardwoods (Eucalyptus and poplar), plantations of clones at different ages (3 trees per age) for the same clone in the same environment have been used for in-situ measurements of maturation strains (Baillères 1994, Gérard 1994, Thibaut et al. 1996). No clear influence of age was found (see data for poplar).

In order to know, a-posteriori, the values of the maturation strains for each ring of a log, the relationships between local maturation strain and wood parameters at trunk periphery were investigated (Thibaut & Gril 2021). Longitudinal shrinkage is a good parameter in case of reaction wood (compression or tension wood). But, until now, no relationship has been established to estimate the maturation strains from wood parameters (cell wall structure of chemical composition) for normal wood, although there are important variations of maturation strain within normal wood around the periphery of the trunk (Jullien et al 2013).

It can be hypothesized that initial fibre length gradient is mainly related to age per se (true juvenility) while adaption is often the dominant causality for *RW*, *SG* and *SM*, and probably also for maturation strain.

3. Material and methods

3.1. Material

Within the framework of a European collaborative programme called “Stresses in beech”, nine beech forests, representative of European forest management, were selected in 5 countries (Austria, Denmark, France, Germany and Switzerland) (Becker & Beimgraben 2001). The age of the selected trees varied from 70 to 200 years. Maturation strain at 8 peripheral positions was measured on 440 standing beech trees from the 9 plots (Jullien et al 2013).

In each plot, 10 trees (86 in total) were selected for the measurement of wood properties. One small log of 50 cm length was cut at a height of 4 m for each tree. Each small log was cut into radial boards, through the pith, from North to South. These boards were air-dried to an average moisture content of 13.5 % (equilibrium at 20°C and 65% RH) and cut into 1259 rods of 20 mm in radial, 20 mm tangential and 360 mm longitudinal direction, from the pith outwards (Fig. 4). Those with irregularities or cracks were discarded.

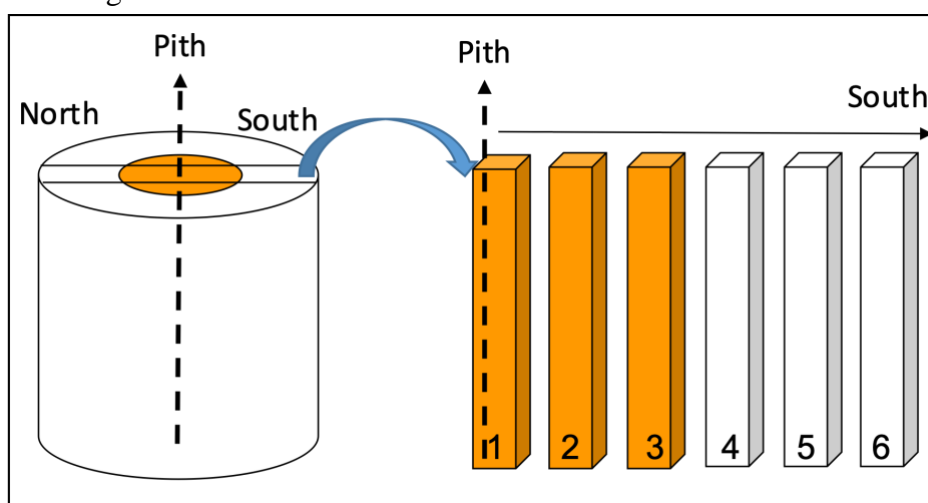


Fig. 4: Diagram of the sawing of the rod after the sawing of a North-South diametrical board. Numbering both for Northern and Southern parts of the board start with pith position. The coloured parts evoke the case of redheart occurrence.

The rods were numbered according to their position in the board and their distance to pith (DP) was measured. At the same time, the number of rings at both ends of the samples was recorded and the mean annual ring width of the rod (RW) was calculated as the ratio of the mean radial dimension to the number of rings. The presence of red heartwood was also noted for the rods located in the core, in relation to a previously published work (Liu et al 2005).

3.2. Measurement of density and specific modulus.

All measurements were done in a regulated room at a temperature of 20°C and a relative humidity of 65%.

The density (D) was calculated by measuring the weight (W) and the dimensions R , T , L of the rod in direction R , T , L , respectively: $D = W/(R.T.L)$. The specific gravity (SG) is the ratio between D and water density.

To measure the specific modulus (SM , $10^6\text{m}^2/\text{s}^2$), each rod is positioned on fine wires and set in free vibration by a hammer stroke. The analysis of the sound vibration by fast Fourier transform gives the values of the three highest resonance frequencies which are interpreted using Timoshenko solution (Brancheriau & Baillères 2002, Brancheriau 2006). The modulus of elasticity (MOE) can be calculated as: $MOE = D.SM$.

3.3. Statistical analysis

Basic statistical analyses were performed using XLSTAT software. The data description table includes the number of data, the minimum, maximum and mean values for each parameter, as well as the coefficient of variation (CV). The normality of the distribution is verified by Shapiro-Wilk test. A Pearson correlation analysis is used in the case of a normal distribution, and a Spearman correlation analysis in the case of a non-normal distribution, which is the majority of cases.

4. Results and discussion

4.1. Radial variations of properties

By giving positive values for the distance to the pith on the North side and negative values on the South side, it is possible to draw the South-North profile of each parameter (RW , SG , SM , MOE) for each tree, as a function of the diametrical position (DP). If there was an increase of the parameter from pith position, the profile is noted “Up”, “Down” for the reverse case and “Flat” when the variation was not clearly up or down. In case of clear asymmetry between the Southern and Northern parts by visual observation, the sample was noted as asymmetric (Fig. 5).

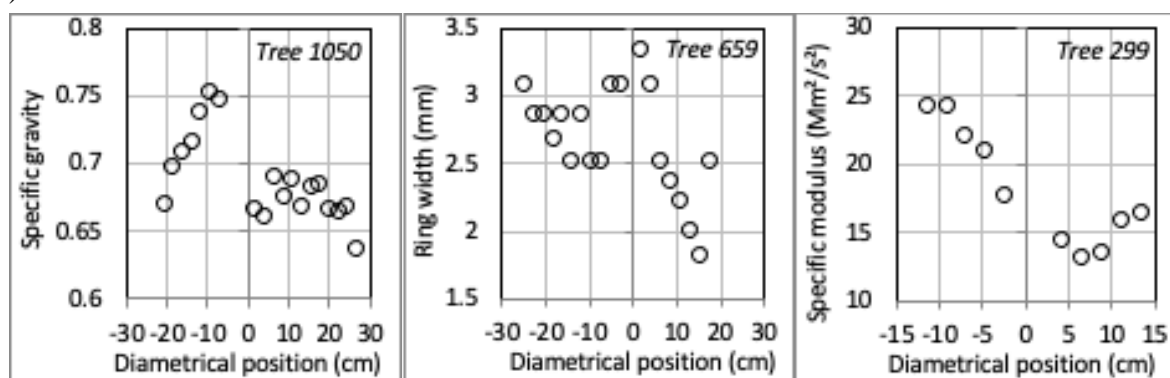


Fig. 5 Examples of clearly asymmetric North-South profiles.

There was a large majority of symmetrical patterns (Table 1).

Table 1 Percentage of profile types per plot within each or wood parameter.

| Para. | Ring width | | | | Density | | | | Specific modulus | | | |
|-------|------------|------|------|------|---------|------|------|------|------------------|-----|------|------|
| PLOT | Up | Down | Flat | Sym | Up | Down | Flat | Sym | PLOT | Up | Down | Flat |
| 1 | 57% | 43% | 0% | 70% | 0% | 25% | 75% | 40% | 1 | 57% | 43% | 0% |
| 2 | 67% | 11% | 22% | 90% | 11% | 0% | 89% | 90% | 2 | 67% | 11% | 22% |
| 3 | 63% | 0% | 38% | 80% | 30% | 0% | 70% | 100% | 3 | 63% | 0% | 38% |
| 4 | 70% | 10% | 20% | 100% | 20% | 0% | 80% | 50% | 4 | 70% | 10% | 20% |
| 5 | 43% | 14% | 43% | 70% | 100% | 0% | 0% | 60% | 5 | 43% | 14% | 43% |
| 6 | 86% | 0% | 14% | 88% | 50% | 0% | 50% | 100% | 6 | 86% | 0% | 14% |
| 7 | 22% | 56% | 22% | 90% | 43% | 14% | 43% | 70% | 7 | 22% | 56% | 22% |
| 8 | 67% | 17% | 17% | 60% | 100% | 0% | 0% | 70% | 8 | 67% | 17% | 17% |
| 9 | 14% | 57% | 29% | 88% | 40% | 0% | 60% | 63% | 9 | 14% | 57% | 29% |
| Mean | 54% | 23% | 23% | 82% | 44% | 4% | 52% | 71% | Mean | 54% | 23% | 23% |

Para.: Wood parameter; Up: initial increase of the parameter from pith to bark; Down: initial decrease of the parameter from pith to bark; Flat: no clear initial increase or decrease; Sym: proportion of globally symmetrical profiles between North and South directions.

Globally there were no noteworthy difference between the Northern and Southern samples (Table 2).

Table 2 Comparison of parameter values North and South.

| Position (Nb) | RW (mm) | SG (kg/m ³) | SM (10 ⁶ m ² /s ²) | MOE (GPa) |
|---------------|---------|-------------------------|--|-----------|
| North (637) | 2.32 | 0.695 | 22.06 | 15.33 |
| South (622) | 2.28 | 0.694 | 22.39 | 15.54 |
| % Sym. | 82% | 71% | 76% | 70% |

RW: mean ring width; SG: mean specific gravity; SM: mean specific modulus;
MOE: mean longitudinal modulus of elasticity; Nb: number of rods;
%Sym: proportion of diametrical patterns considered symmetrical for each parameter.

In each case, the occurrence of rods for each successive radial position within the trees or plots was examined (Fig. 6). Up to 18 cm from the pith, all the plots are concerned and there are always more than 70% of the trees concerned, values lower than 100% being due to defect occurrence close to the pith. This proportion decreases rapidly for larger distances from the pith, due to variable log size. It is therefore preferable not to use rods with a radial distance of more than 18 cm to calculate the mean values of the parameters at the global scale.

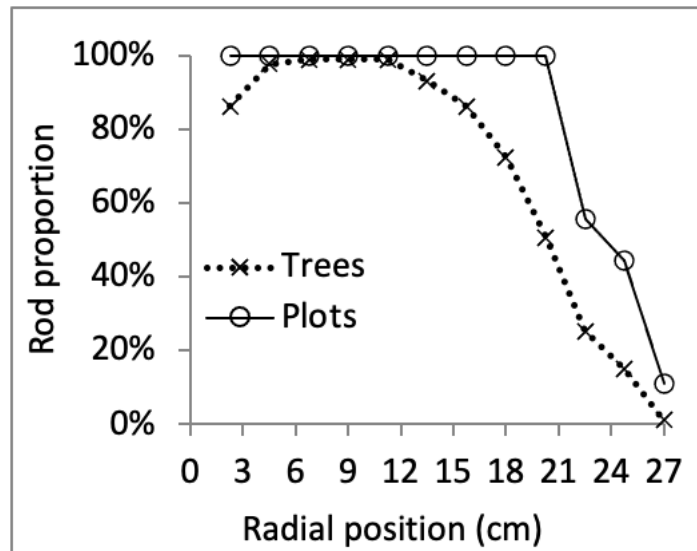


Fig. 6 Percentage occurrence of rods for each successive radial position within trees or plots
100% means that there are used rods at a given radial position in every tree or every plot.

There are notable differences between trees for each parameter, both in value and in pattern. Globally, there is no significant difference between the Northern and Southern samples (Fig. 7). It is thus allowable to mix the beech rods of the Northern and Southern specimens for further analysis of the mean radial variation patterns at the global or plot level.

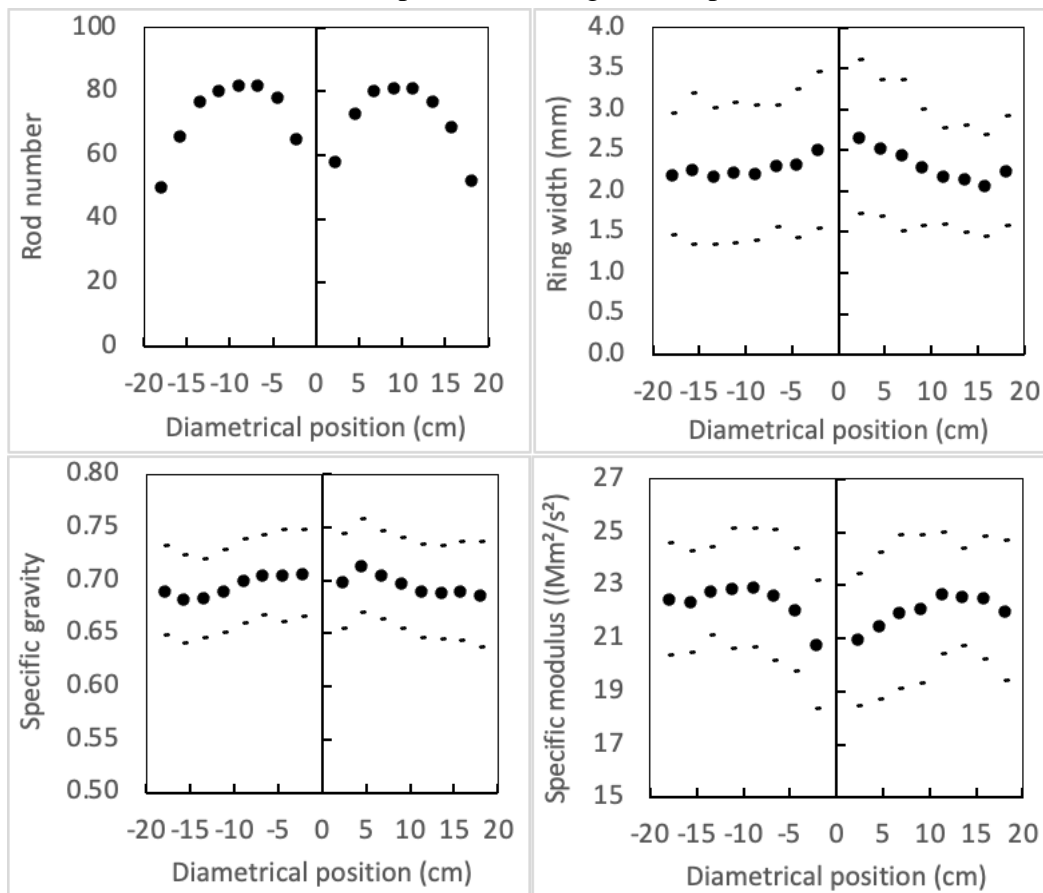


Fig. 7 Number of rods and parameter values for all trees as a function of diametrical position (DP)
Bolt dots: mean value; thin dashes: mean value + or – standard deviation.

Moreover, some trees have a part of red core-wood portion and the effect it may have on properties was investigated. All trees (25) without any red rod (except sometimes one near the pith) were considered as white beech while all trees with more than two red rods were considered as red beech. The mean radial variations for red and white beech trees were calculated (Fig. 8). Due to the variability between the trees, no clear difference could be observed between the mechanical properties of red and white beech wood.

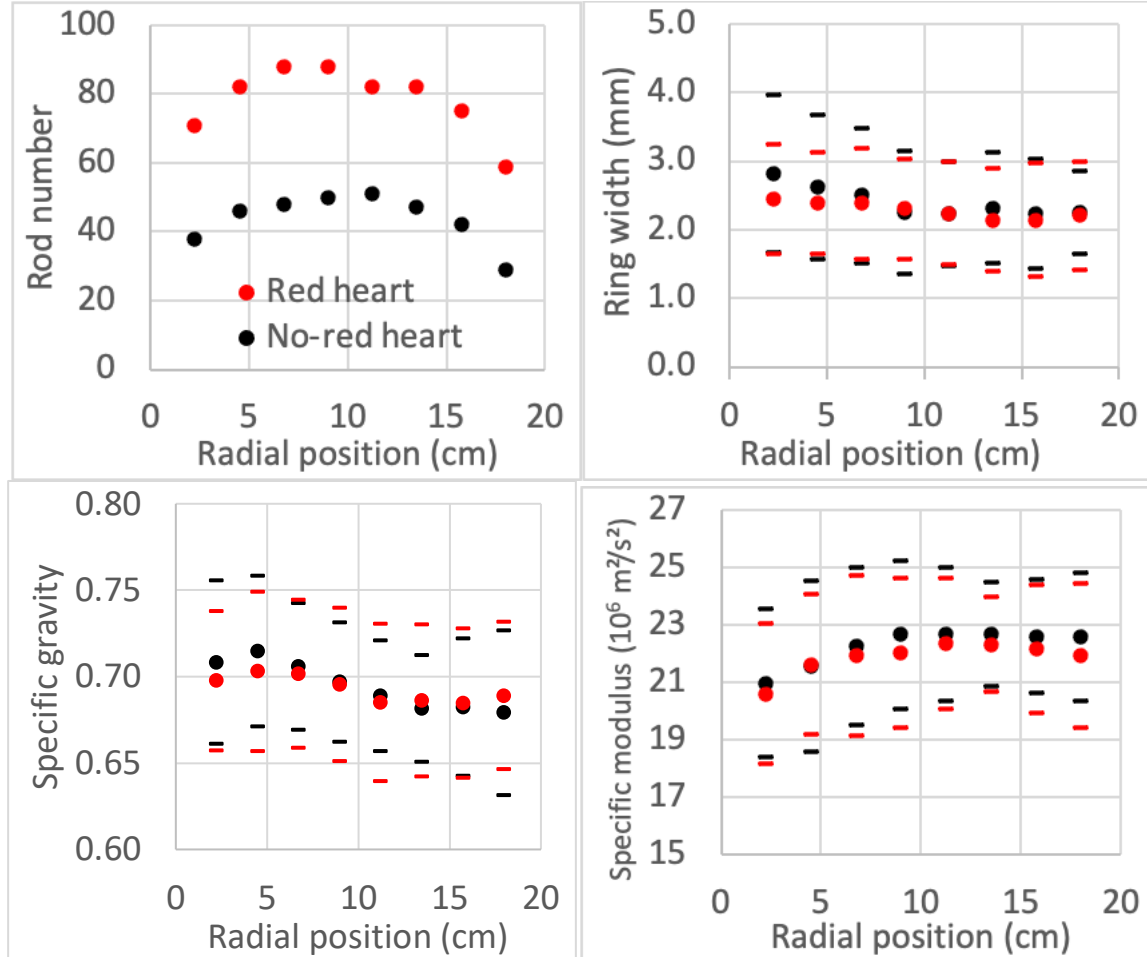


Fig. 8 Values of parameter for all red and no-red hearted trees as a function of radial position.

Bolt dots: mean value; thin dashes: mean value + or – standard deviation.

Red dots: red heartwood; black dots white heartwood

It is thus allowable to mix Northern and Southern specimens of red and white beech rods for further analysis of the mean radial variation patterns at the global or plot level.

The global mean radial patterns for these beech trees were as follows (Fig. 9):

- *RW* decreases regularly (2.6 to 2.2 mm) from pith to bark;
- *SG* increases a little (0.703 to 0.709) at the beginning (up to about 4 cm radius) and decreases thereafter (0.709 to 0.686), but the variations are small;
- *SM* increases (20.8 to 22.8 m²/s) for a rather long time (up to about 12 cm radius) and then decreases (22.8 to 22.2 m²/s²) regularly;
- the *MOE* pattern is very similar to the *SM* pattern.

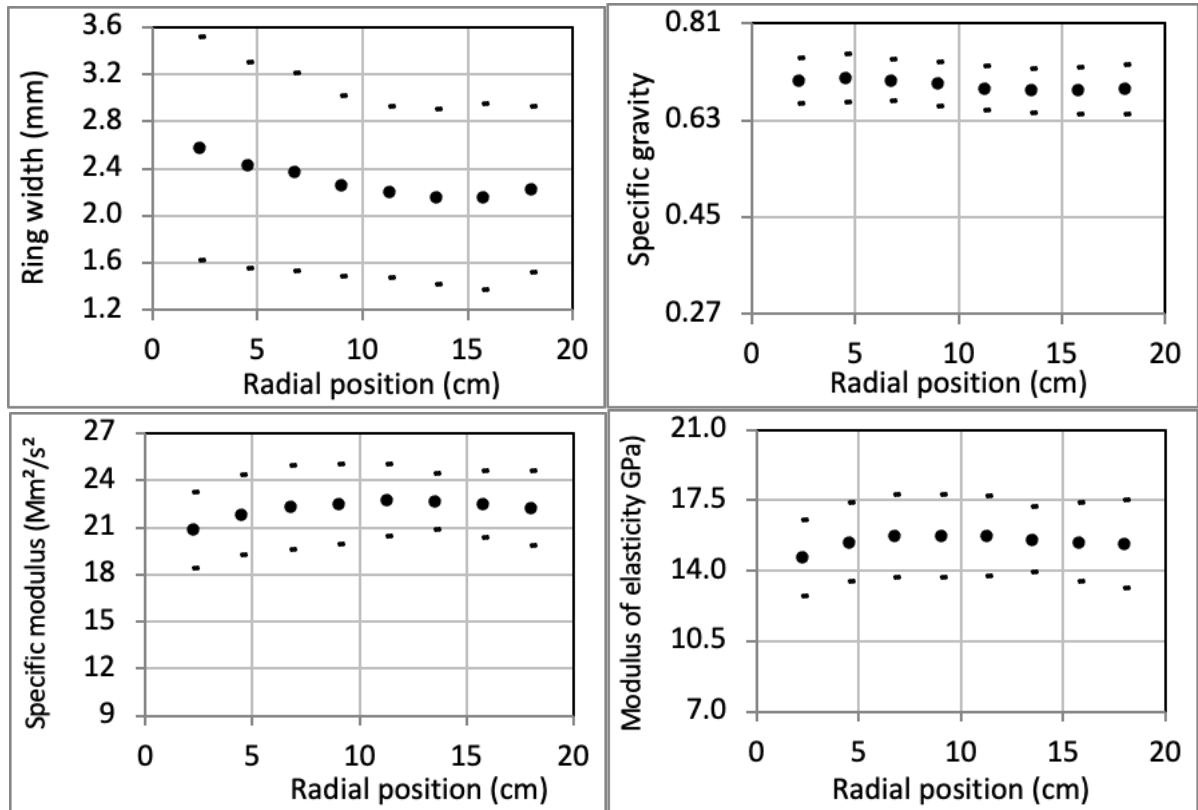


Fig. 9 Mean radial distribution of indicators and modulus of elasticity for all rods.

Bolt dots: mean value; thin dashes: mean value + or – standard deviation.

A ratio of 3 has been set for all graphs between maximum and minimum values of the ordinate axis.

The variability between trees (standard deviation values) is high for *RW* but low for *SG*. It is slightly higher for *SM* and *MOE* (Table 6).

The mean patterns of the plots (Fig. 10) are more irregular due to the smaller number of rods, but, more or less, the global mean pattern is the most frequent. There are differences between plots, in the mean level of properties and sometimes in the pattern, mainly for *RW*, with some plots having increasing *RW* (plot 7 and 9).

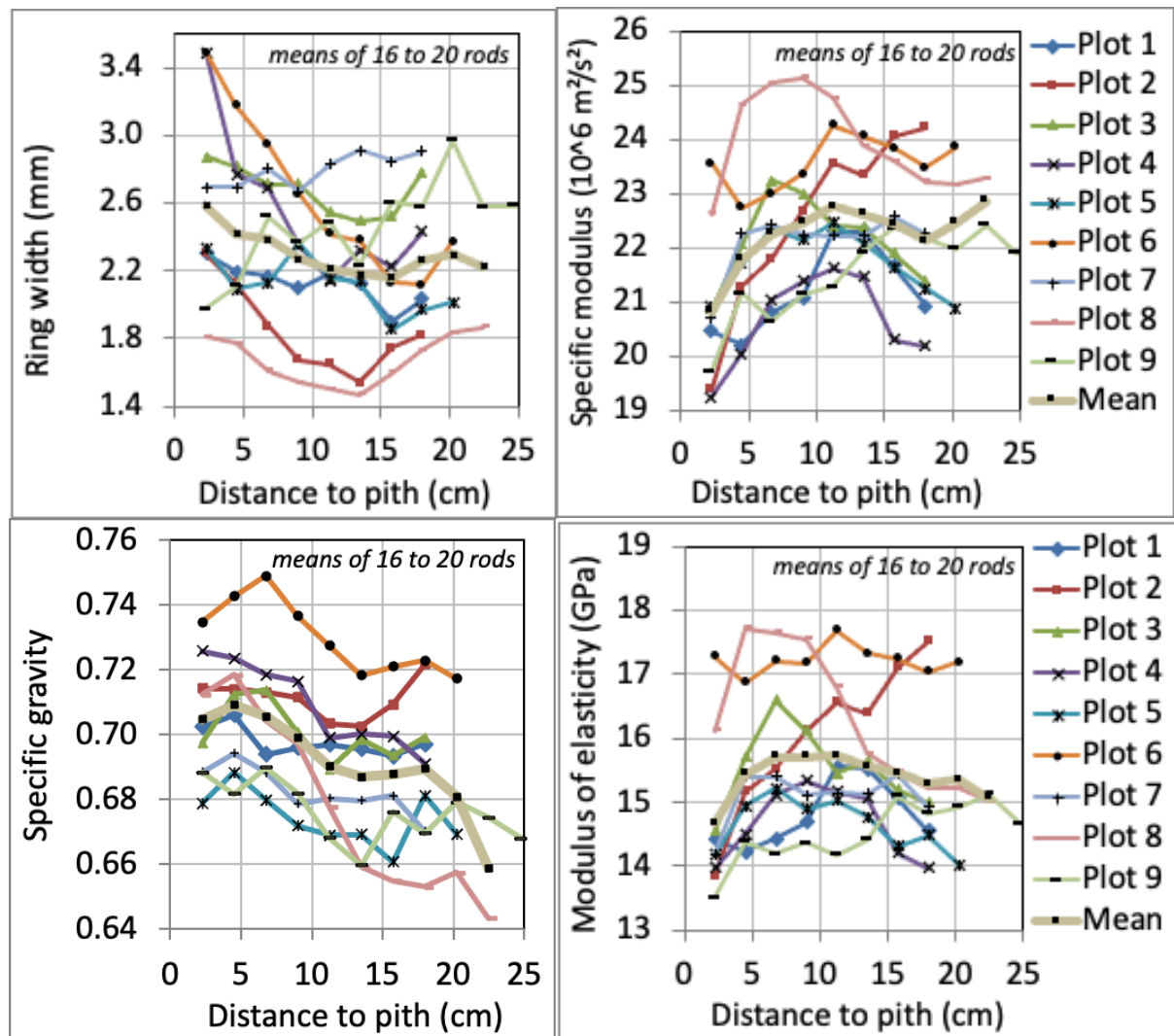


Fig. 10 Mean radial variations of properties at the plot level
Mean: mean values for all rods at each radial position.

It is interesting to look at the evolution of the ring surface from pith to bark, using the radial position ($PoRa$) and the mean ring width of each rod:

$$RSra = 2\pi.PoRa.RW$$

The evolution of the mean values of all $RSra$ at the same radial position for all trees in a plot, from pith to bark (Fig. 11), is a signature of the trunk surface growth for the plot. For these beech plots, the ring surface can be considered proportional to the distance from the pith with a regression coefficient (R^2) always above 0.96 (Table 3):

$$RSra = K.PoRa$$

K has a mean value of 1.43 cm²/cm, and ranges from 1.09 to 1.88. This kind of linear growth quasi proportional to distance to pith together with K values can be considered as a result of forest management in these European plots.

Table 3 Proportional coefficient (K) and R^2 values for linear regressions

| Plot | 1 | 2 | 3 | 4 | 5 | 6 | 7 | 8 | 9 | Mean |
|-------|------|------|------|------|------|------|------|------|------|------|
| K | 1.25 | 1.14 | 1.69 | 1.47 | 1.28 | 1.44 | 1.88 | 1.09 | 1.63 | 1.43 |
| R^2 | 0.98 | 0.96 | 0.99 | 0.98 | 0.98 | 0.96 | 0.98 | 0.98 | 0.98 | 0.99 |

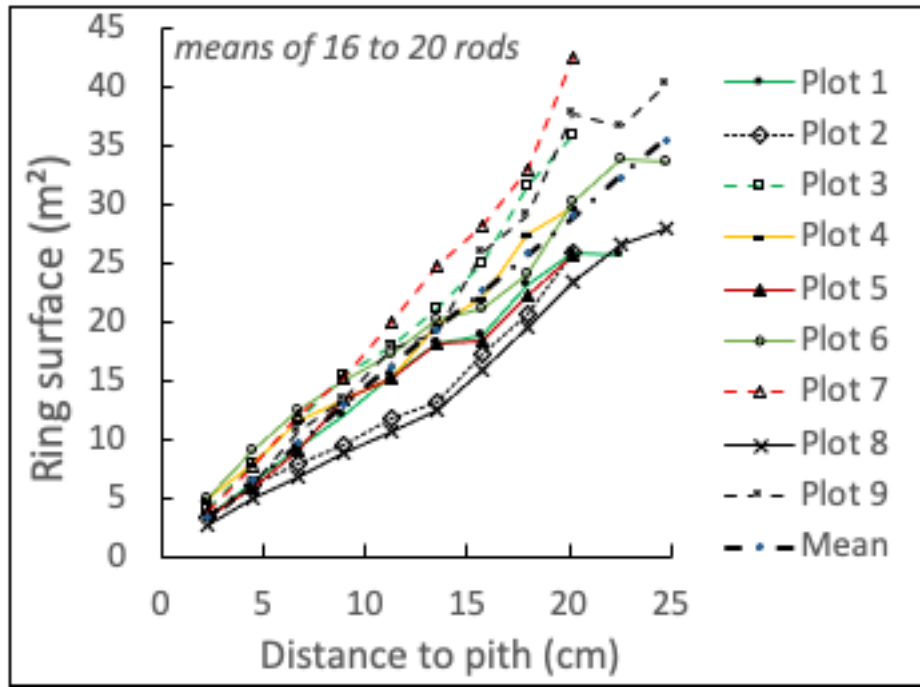


Fig. 11 Variation of ring surface (cm²) with distance to pith (cm) for each plot.
Mean: regression for mean values

4.2. Global results

4.2.1. Global results at rod level

Table 4 and 5 give global description and correlation within the data for all samples (1259 rods).

Table 4 Parameter description for all rods

| 1259 rods | RW | SG | SM | MOE |
|-----------|-------|------|-------|-------|
| Minimum | 0.67 | 0.55 | 11.08 | 8.00 |
| Maximum | 6.67 | 0.83 | 27.49 | 21.30 |
| Mean | 2.30 | 0.69 | 22.22 | 15.44 |
| Max/min | 10.00 | 1.51 | 2.48 | 2.66 |
| C. V. | 35.0% | 6.2% | 10.9% | 13.0% |

RW (mm): ring width; *SG*: specific gravity; *SM* (10⁶m²/s²): specific modulus;
MOE (GPa): longitudinal modulus of elasticity.

The variations of *SG* between samples are very low (coefficient of variation 6%).

Table 5 Correlation table for all rods

| 1259 rods | RW | SG | SM | MOE |
|-----------|--------|-------|--------|--------|
| RW | 1 | 0.215 | -0.313 | -0.167 |
| SG | 0.215 | 1 | 0.047 | 0.506 |
| SM | -0.313 | 0.047 | 1 | 0.884 |
| MOE | -0.167 | 0.506 | 0.884 | 1 |

RW: ring width; *SG*: specific gravity; *SM*: specific modulus; *MOE*: longitudinal modulus of elasticity.

Bold numbers: correlation significant at 0.1% level.

There is no significant correlation (at the 5% level) between *SG* and *SM*. *RW* has a very significant correlation (at the 0.1% level) positively with *SG* and negatively with *SM*. Thus, the correlation between *RW* and *MOE* is negative with a lower coefficient of determination (3%). In the determination of *MOE* from *SM* and *SG*, the coefficient of determination (square of the correlation coefficient given in Table 5) is three times higher for *SM* (78%) than for *SG* (26%).

4.2.2. Global results at tree level

Tables 6 and 7 give the description and correlation table for tree dimension and mean per tree. Variability of parameters is significantly lower for tree mean values, and notably low for *SG*.

Table 6 Parameter description for tree mean values

| 86 trees | RW | D | SM | MOE |
|----------|-------|------|------|------|
| Minimum | 1.29 | 0.63 | 17.6 | 12.0 |
| Maximum | 4.78 | 0.78 | 25.6 | 19.3 |
| Mean | 2.28 | 0.70 | 22.4 | 15.6 |
| Max/min | 3.70 | 1.24 | 1.46 | 1.60 |
| C.V. | 24.9% | 4.8% | 7.6% | 9.5% |

RW (mm): ring width; *SG*: specific gravity; *SM* ($10^6\text{m}^2/\text{s}^2$): specific modulus; *MOE* (GPa): longitudinal modulus of elasticity.

Except for *RW*, the mean wood properties per tree show rather low variations between trees (very low for *SG*).

Table 7 Correlation table for all trees

| 86 Trees | RW | D | SM | MOE |
|----------|--------|-------|--------|--------|
| RW | 1 | 0.122 | -0.388 | -0.252 |
| D | 0.122 | 1 | 0.140 | 0.602 |
| SM | -0.388 | 0.140 | 1 | 0.874 |
| MOE | -0.252 | 0.602 | 0.874 | 1 |

RW: ring width; *SG*: specific gravity; *SM*: specific modulus; *MOE*: longitudinal modulus of elasticity.
Bold numbers: correlation significant at 0.1% level.

Among the wood properties, *RW* and *SM*, *SM* and *MOE*, *SG* and *MOE* remain highly significantly correlated (0.1% level) at the tree level.

4.2.3. Global results at plot level

Table 8 gives the description of tree dimensions and mean wood properties per tree for the 9 forest plots and Table 9 the correlation table for all plots. Except for *RW*, the mean wood properties per plot all show very little variation between plots.

Table 8 Parameter description for the 9 plots mean values

| Plot | Nb trees | RW | D | SM | MOE |
|------|----------|------|------|------|------|
| 1 | 10 | 2.06 | 0.70 | 21.5 | 15.0 |
| 2 | 10 | 1.80 | 0.71 | 23.1 | 16.4 |
| 3 | 10 | 2.63 | 0.70 | 22.2 | 15.6 |
| 4 | 10 | 2.50 | 0.71 | 21.2 | 15.1 |
| 5 | 10 | 2.12 | 0.68 | 21.9 | 14.8 |
| 6 | 8 | 2.57 | 0.73 | 23.7 | 17.3 |

| | | | | | |
|---------|----|-------|------|------|------|
| 7 | 10 | 2.84 | 0.68 | 22.0 | 15.1 |
| 8 | 10 | 1.63 | 0.68 | 24.1 | 16.4 |
| 9 | 8 | 2.50 | 0.67 | 21.7 | 14.6 |
| Max | | 2.8 | 0.7 | 24.1 | 17.3 |
| Min | | 1.6 | 0.7 | 21.2 | 14.6 |
| Mean | | 2.29 | 0.70 | 22.4 | 15.6 |
| Max/min | | 1.74 | 1.08 | 1.14 | 1.18 |
| CV | | 16.9% | 2.6% | 4.2% | 5.5% |

RW (mm): ring width; *SG*: specific gravity; *SM* ($10^6\text{m}^2/\text{s}^2$): specific modulus; *MOE* (GPa): longitudinal modulus of elasticity.

At the plot mean level, only the causal relationship between *MOE* and *SG* or between *MOE* and *SM* remains significant at the 0.1% level (Table 9).

Table 9 Correlation table for all plots

| 9 Plots | RW | D | SM | MOE |
|---------|--------|-------|--------|--------|
| RW | 1 | 0.154 | -0.446 | -0.266 |
| D | 0.154 | 1 | 0.252 | 0.671 |
| SM | -0.446 | 0.252 | 1 | 0.886 |
| MOE | -0.266 | 0.671 | 0.886 | 1 |

RW: ring width; *SG*: specific gravity; *SM*: specific modulus; *MOE*: longitudinal modulus of elasticity.
Bold numbers: correlation significant at 0.1% level.

4.3. Pre-stressing and growth forces

In situ measurements on standing trees give values of *GSI* for North and South sides at breast height for each tree (Jullien et al 2013). *RW*, *SG* and *SM* values are measured in laboratory for the last rods (farthest away from pith) at North and South positions and 4 m high in the tree. We can expect that these 3 wood parameters are good estimations for the values at breast height level.

All the North and South values labelled with the subscript _{last} for wood parameters were gathered in the same sheet (Maturation): distance to pith (DP_{last} in cm), ring width (RW_{last} in mm), specific modulus (SM_{last} in $10^6\text{m}^2/\text{s}^2$), longitudinal modulus of elasticity (MOE_{last} in GPa) of the last rod (North & South), *GSI* (North & South) for the 86 trees.

Firstly, the calculation of maturation stress (pre-stressing value) and growth force needs green wood values for parameters such as *DP*, *RW* and *MOE*. In the literature (Cirad 2015) we can find a mean value for radial shrinkage ($RS=5.7\%$) and fibre saturation point ($FSP=32\%$) of beech wood. The moisture content of the rods was 13.5%, which is 18.5% below *FSP*. The increase in radial dimension between the air-dry and green state of the wood can be estimated by the shrinkage proportion (*PS*):

$$PS = 5.7\% \times 18.5\% / 32\% = 3.3\%$$

Thus the width of the green ring (RW_g) and green distance to pith (DP_g) can be obtained from the air dry values (*RW* and *DP*) by the formulas:

$$RW_g = 1.033 RW : DP_g = 1.033 DP$$

and ring portion surface (RS_g) is calculated as $RS_g = \Delta\theta \times DP_g \times RW_g$, where the angular sector $\Delta\theta$ corresponding to a given *GSI* value is taken as $\pi/4$.

Air dry (MOE) and green (MOE_g) longitudinal modulus of elasticity are proportional according to the formula (Thibaut & Gril 2021):

$$MOE_g = 0.8943 \times MOE$$

It is also necessary to convert GSI values into maturation strains (α_m) using the conversion factor FI (Thibaut & Gril 2021):

$$\alpha_m = FI \times GSI$$

FI can be calculated from the formula:

$$FI = -0.475 \times SM_b + 25.24$$

SM_b is the basic specific modulus which is proportional to the specific modulus SM (Thibaut & Gril 2021):

$$SM_b = 1.1068 \times SM; \text{ so } FI = -0.5257 \times SM + 25.24$$

Using the values of the maturation strain α_m and green MOE , the value of the maturation stress (which is the value of the tensile pre-stress at the periphery of the trunk) can be calculated:

$$\sigma_m = MOE_g \times \alpha_m$$

Then, the local force generated on the unit ring portion (ΔF in N) by the maturation process can be calculated:

$$\Delta F = RS_g \times \sigma_m$$

For the 3 explaining factors (RS_g , MOE_g , GSI), the variability is rather low for MOE , high for local ring surface and very high for GSI . Thus it is also very high for local maturation strain, maturation stress (pre-stressing value) and growth force (Table 10).

Table 10 Statistical description of maturation parameters

| | ΔS_g | MOE_g | GSI | FI | α_m | σ_m | ΔF |
|---------|--------------|---------|-------|------|------------|------------|------------|
| Mean | 4.04 | 13.7 | 83 | 13.6 | 1109 | 15.4 | 6025 |
| Median | 3.60 | 13.9 | 70 | 13.4 | 941 | 12.3 | 4335 |
| Minimum | 0.77 | 8.4 | 0 | 10.8 | 0 | 0.0 | 0 |
| Maximum | 10.80 | 19.1 | 251 | 18.6 | 3103 | 47.6 | 23342 |
| CV | 45% | 15% | 68% | 10% | 66% | 70% | 79% |

RS_g (cm²): local ring surface; MOE_g (GPa): longitudinal modulus of elasticity of the last ring;

GSI (μm) growth stress indicator measured in situ on standing tree;

FI conversion factor between GSI and maturation strain; α_m : maturation strain (10^{-6});

σ_m (MPa): maturation stress; ΔF (N): local growth force. CV: coefficient of variation.

Both pre-stressing and growth force are strongly related to maturation strain ($R^2 = 92\%$ and 62% respectively) through proportional laws. Growth force and pre-stressing are very significantly correlated but 35% of growth forces variations are not explained by pre-stressing variations (Fig. 12).

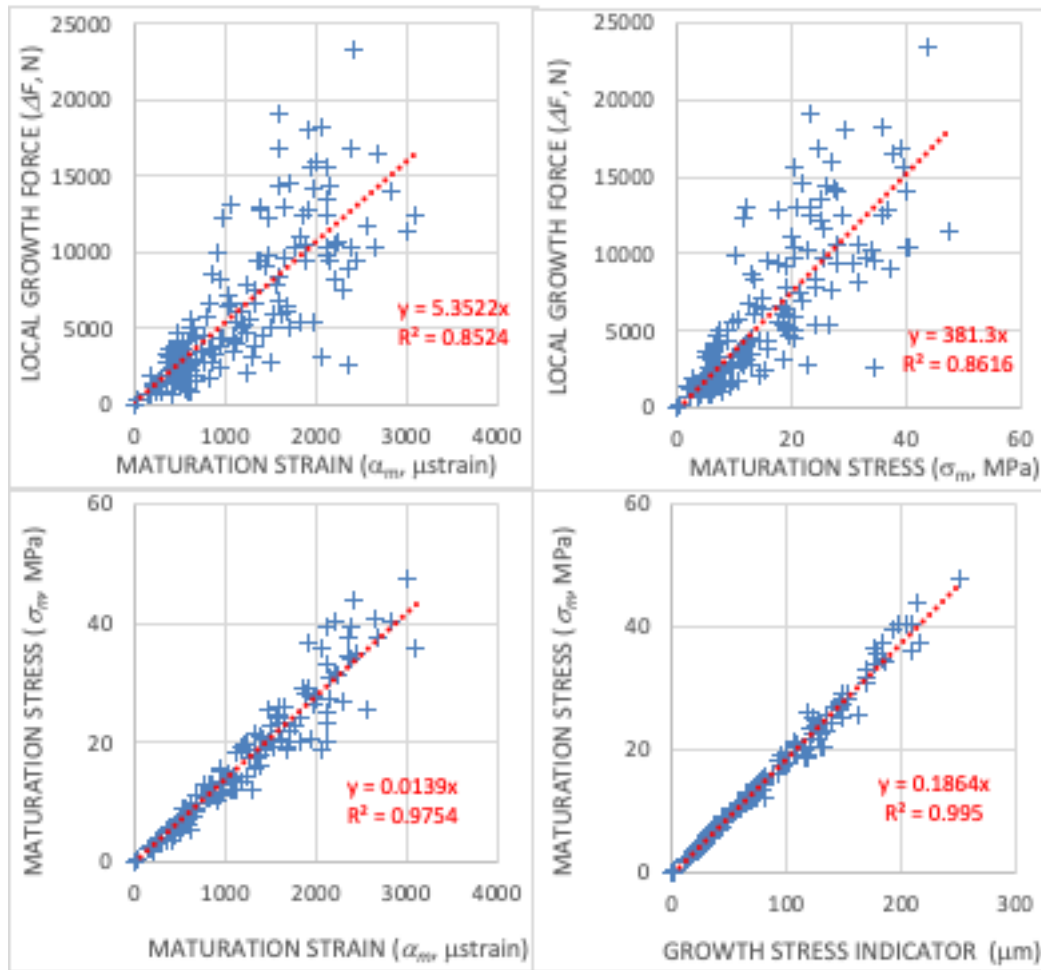


Fig 12: Relationships between growth forces, maturation strain or growth stress indicator, and maturation stress.

4.4. Discussion and conclusion

There are few published results relating to radial variations of mechanical parameters in large trees of high forests that are not the result of plantation. In Europe, old growth beech forests can have different forest origins: i) even-aged (France or Germany) or uneven-aged high forest (Switzerland), coppicing with standards (France) or conversion of coppice forest into high forest (Ciancio et al 2006) (Germany, France) but are very rarely the result of plantations (none in the 9 plots). *Fagus* is known for its shade tolerance and ability to grow very slowly under a closed canopy (Collet et al 2011) and most forest plots undergo more or less severe thinning before final harvesting, which leads to an increase of *RW* due to better access to light (Noyer et al 2017). This is reflected in the different mean *RW* radial patterns for the 9 plots (Fig. 10). For plots 7 and 9, a clear increase of *RW* is observed in the young ages, while the reverse and classical pattern is true for plots 2, 4 and 6. Similar results were found on younger beech trees (Bouriaud et al 2004).

As a mean for these high forest beech trees, the radial patterns of variations are partly similar to the typical radial pattern for *RW* and *SM*. *SG* has a very small decreasing variation. But looking tree by tree, there are all types of patterns (increasing or decreasing at the beginning) for all parameters (*RW*, *SG* and *SM*). This supports the hypothesis of an “adaptation” for “mechanical” juvenility.

Due to the very low variability of the *SG* of beech wood, the variations of *SM* are much more important than those of *SG* in order to explain the variations of *MOE*.

The high level of inter-tree variability (CV=66%) for pre-stressing (σ_m) is massively due to variations in maturation strains combined with variations in *MOE*, while for growth forces (ΔF), the high level of variability between trees (CV=79%) is also mainly linked to variations in maturation strains combined with variations in local ring surface and *MOE* (Table 11). Although growth force and maturation stress are very significantly linked ($R^2 = 64\%$) due to the influence of the maturation strain, the ring width has no influence on pre-stressing and appears to be a possible trade-off parameter between the two mechanical functions of growth forces: pre-stressing of trunk periphery and posture control of axis position.

Table 11 Contribution of several factors to the variance of local growth force and maturation stress

| R^2 | α_m | MOE_g | DP_{last} | RW_{last} | RS_g |
|------------|------------|---------|-------------|-------------|--------|
| ΔF | 61.8% | 5.0% | 9.4% | 11.7% | 17.2% |
| σ_m | 92.5% | 11.6% | 0.4% | 0.6% | 0.9% |

R^2 : coefficient of determination; ΔF : local growth force; σ_m : maturation stress; α_m : maturation strain; MOE_g : modulus of elasticity in green state; DP_{last} : distance to pith of last ring; RW_{last} : width of last ring; RS_g : ring portion surface.

Acknowledgments

The data were obtained thanks to the support of European Commission through the FAIR-project CT 98-3606, coordinated by Prof. Gero Becker. The financial support of CNRS K. C. Wong post-doctoral program and China Scholarship Council must be also acknowledged.

References

- Alméras T, Thibaut A, Gril J. 2005. Effect of circumferential heterogeneity of wood maturation strain, modulus of elasticity and radial growth on the regulation of stem orientation in trees. *Trees Structure and function* 19 (4), 457-467. <https://doi.org/10.1007/s00468-005-0407-6>
- Alméras T, Fournier M. 2009. Biomechanical design and long-term stability of trees: Morphological and wood traits involved in the balance between weight increase and the gravitropic reaction. *Journal of Theoretical Biology* 256: 370–381. <https://doi.org/10.1016/j.jtbi.2008.10.011>
- Alméras T, Clair B. 2016. Critical review on the mechanisms of maturation stress generation in trees. *Journal of the Royal Society, Interface* 13(122), 20160550. <https://doi.org/10.1098/rsif.2016.0550>
- Baillères H.. 1994. Précontraintes de croissance et propriétés mécano-physiques de clones d'Eucalyptus (Pointe Noire, Congo) : hétérogénéités, corrélations et interprétations histologiques. Thèse en sciences du bois, Université Bordeaux 1 (In French). <https://www.theses.fr/1994BOR10521>
- Bao FC, Jiang ZH, Jiang XM, Lu XX, Luo XQ, Zhang SY. 2001. Differences in wood properties between juvenile wood and mature wood in 10 species grown in China. *Wood Science and Technology* 35:363-375. <https://doi.org/10.1007/s002260100099>
- Bhat KM, Priya PB, Rugmini P. 2001. Characterisation of juvenile wood in teak. *Wood Science and Technology* 34:517-532. <https://doi.org/10.1007/s002260000067>
- Becker G, Beimgraben T. 2001. Occurrence and relevance of growth stresses in Beech (*Fagus sylvatica* L.) in Central Europe. Final Report of FAIR-project CT 98-3606, Coordinator Prof. G. Becker, Institut für Forstbenutzung und forstliche Arbeitwissenschaft, Albert-Ludwigs Universität, Freiburg, Germany

- Bendtsen BA, Senft J. 1986. Mechanical and anatomical properties in individual growth rings of plantation-grown eastern cottonwood and Loblolly pine. *Wood and Fiber Science* 18(1): 23-38
- Bouriaud O, Bréda N, Le Moguédec G, Nepveu G. 2004. Modelling variability of wood specific gravity in beech as affected by ring age, radial growth and climate. *Trees* 18:264–276. <https://doi.org/10.1007/s00468-003-0303-x>
- Brancheriau L, Baillères H. 2002. Natural vibration analysis of wooden beams: a theoretical review. *Wood Science and Technology*, 36(4):347-365. <https://doi.org/10.1007/s00226-002-0143-7>
- Brancheriau L. 2006. Influence of cross section dimensions on the Timoshenko's shear factor – Application to wooden beams in free-free flexural vibration. *Annals of Forest Science*, 63(3):319-321. <https://doi.org/10.1051/forest:2006011>
- Ciancio O, Corona P, Lamonaca A, Portoghesi L, Travaglini D. 2006. Conversion of clearcut beech coppices into high forests with continuous cover: A case study in central Italy. *Forest Ecology and Management* 224: 235–240. <https://doi.org/10.1016/j.foreco.2005.12.045>
- Cirad 2015. Tropix®7: The main technological characteristics of 245 tropical wood species. Cirad Montpellier, France. <https://doi:10.18167/74726F706978>
- Collet C, Fournier M, Ningre F, Hounzandji AP, Constant T. 2011. Growth and posture control strategies in *Fagus sylvatica* and *Acer pseudoplatanus* saplings in response to canopy disturbance. *Annals of Botany* 107, 1345–1353. <https://doi.org/10.1093/aob/mcr058>
- Cown D, Dowling L. 2015. Juvenile wood and its implications. *NZ Journal of Forestry*, February 2015, Vol. 59, No. 4: 10-17
- Fournier M, Bordonné PA, Guitard D, Okuyama T. 1990. Growth stress patterns in living stems – A model assuming evolution with the tree age of maturation strains. *Wood Science and Technology* 24: 131-142. <https://doi.org/10.1007/BF00229049>
- Fournier M, Chanson B, Thibaut B, Guitard D. 1991. Mechanics of standing trees: modelling a growing structure subjected to continuous and fluctuating loads. 2. Three-dimensional analysis of maturation stresses in a standard broadleaved tree. *Annales des Sciences Forestières* 48, 527-546 (in French). <https://doi.org/10.1051/forest:19910504>
- Fournier M, Chanson B, Thibaut B, Guitard D. 1994. Measurements of residual growth strains at the stem surface, in relation to its morphology. Observations on different species. *Annales des Sciences Forestières* 51, 249-266. <https://doi.org/10.1051/forest:19940305>
- Gérard J. 1994. Contraintes de croissance, variations internes de densité et déformations de sciage chez les eucalyptus de plantation. Thèse de doctorat, Université de Bordeaux 1, Sciences du bois.
- Jullien D, Widmann R, Loup C, Thibaut B. 2013. Relationship between tree morphology and growth stress in mature European beech stands. *Annals of forest science* 70 (2), 133-142. <https://doi.org/10.1007/s13595-012-0247-7>
- Kojima M, Yamamoto H, Yoshida M, Ojio Y, Okumura K. 2009. Maturation property of fast-growing hardwood plantation species: A view of fiber length. *Forest Ecology and Management* 257: 15–22. <https://doi.org/10.1016/j.foreco.2008.08.012>
- Kollmann FF, Côté WA. 1968. Principles of Wood Science and Technology. I – SolidWood, Springer, New York, 592 p.
- Koubaa A, Hernandez RE, Baudouin M, Poliquin J. 1998. Inter clonal, intra clonal and within-tree variation of fiber length of poplar hybrid clones. *Wood and Fiber Science* 30(1): 40-47

Kretschmann DE. 2010. Mechanical properties of wood. In Wood handbook: Wood as an engineering material. General Technical Report FPL-GTR-190. Madison: Forest Products Laboratory, USDA, Forest Service.

Lachenbruch B, Moore J, Evans R. 2011. Radial variation in wood structure and function in woody plants, and hypotheses for its occurrence. In: Meinzer FC, Lachenbruch B, Dawson TE (eds) Size- and age-related changes in tree structure and function. Springer, Dordrecht: 121–164.

Larson PR, Kretschmann DE, Clark III A, Isebrands JG. 2001 Formation and properties of juvenile wood in southern pines - A synopsis. USDA forest service, FPL-GTR–129

Liu S, Loup C, Gril J, Dumonceaud O, Thibaut A, Thibaut B. 2005. Studies on European beech (*Fagus sylvatica* L.): variations of colour parameters. *Annals of Forest Science*, 62: 625-632. <https://doi.org/10.1051/forest:2005063>

Mc Lean JP, Zhang T, Bardet S, Beauchêne J, Thibaut A, Clair B, Thibaut B. 2011. The decreasing radial wood stiffness pattern of some tropical trees growing in the primary forest is reversed and increases when they are grown in a plantation. *Annals of Forest Science* 68: 681-688. <https://doi.org/10.1007/s13595-011-0085-z>

Noyer E, Lachenbruch B, Dlouhá J, Collet C, Ruelle J, Ningre F, Fournier M. 2017. Xylem traits in European beech (*Fagus sylvatica* L.) display a large plasticity in response to canopy release. *Annals of Forest Science* 74: 46, <https://doi.org/10.1007/s13595-017-0634-1>

Raven PH, Evert RF, Eichhorn SE. 2007. The biology of plants. Brussels: De Boeck.

Savidge RA. 2003. Tree growth and wood quality. In: Wood quality and its biological basis, edited by JR. Barnett and G. Jeronimidis, Blackwell scientific, Oxford, UK (ISBN: 978-1-405-14781-1): 1-29

Thibaut B. 2019. Three-dimensional printing, muscles and skeleton: mechanical functions of living wood, *Journal of Experimental Botany*, Volume 70, Issue 14, 1 July 2019, Pages 3453–3466. <https://doi.org/10.1093/jxb/erz153>

Thibaut B, Gril J, Fournier M. 2001. Mechanics of wood and trees, some new highlights for an old story. *Comptes Rendus de l'Académie des Sciences Paris, Série II B* 329, 701–716.

Thibaut B, Gril J. 2021. Tree growth forces and wood properties. *Peer Community Journal*, Volume 1 (2021), article no. e46. <https://doi.org/10.24072/pcjournal.48>

Thibaut B, Paillassa E, Fournier M, Castera P, Sassus F. 1996. – Etude de la fente à l'abattage du peuplier et du bois de tension, pour mieux comprendre ce phénomène et réduire les pertes qu'il provoque, Rapport final contrat "Agriculture Demain" MRT 92.G.0363, 7.96.